MSUCL-179
July 1975

An Ultra Thin ΔE-E Counter Telescope with Position Sensitivity in Two Dimensions*

R.G. Markham, Sam M. Austin and H. Laumer+

Cyclotron Laboratory and Physics Department
Michigan State University, East Lansing, Michigan 48824

ABSTRACT

A thin-window proportional counter(ΔE)-Si surface barrier detector(E) telescope is described which has position sensitivity in two dimensions with a resolution of <0.40 mm FWHM (σ_{rms}<0.17 mm). The counter is well suited for particles with E/M=0.2 to 5 MeV/amu and is very easy to construct and to use.

* Supported by the U.S. National Science Foundation.

+ Present address: Physics Department, University of Kentucky, Lexington, Kentucky 40506

1. Introduction

Counter telescopes consisting of a gas proportional counter for ΔE and a Si surface barrier detector for E are certainly not new; however, their full potential has seldom been exploited. Here we describe a compact version of such a detector with the following major characteristics: Simple construction, spatial resolution of less than 0.4 mm FWHM in two dimensions, ΔE resolution of 7% plus straggling, energy and time resolution characteristic of a surface barrier detector and thin windows allowing detection of particles with energy as low as E/M=0.2 MeV/amu. The performance of three common gases with respect to position resolution is investigated.

Two systems with somewhat similar characteristics have been reported recently. One of these is a proportional counter having two dimensional position sensitivity with resolution <0.4 mm FWHM.[1] However the extensive use of field shaping wires makes this type of counter unusable as a ΔE detector in a telescope requiring good ΔE and E resolution. A position sensitive ionization chamber has also been reported[2] which gives good ΔE and E resolution. This detector is, however, quite complex and gives relatively poor position and time resolution.

2. Construction

A schematic drawing and photograph of the counter are shown in Figs. 1 and 2. The body of the detector is machined from aluminum and houses the surface barrier detector (Ortec 400 mm^2 heavy-ion type) and the proportional counter chamber. The surface barrier detector is held in place by its rear-mounted Microdot

connector which is mated with a vacuum feedthrough. The front face of the surface barrier detector serves as the rear cathode of the proportional counter whose anode wire* is mounted (on wire extensions of standard BNC vacuum feedthroughs) just outside the active volume.

Two types of windows have been employed. The simplest were gold coated mylar foils as thin as 300 $\mu g/cm^2$. Very much thinner windows have been made from multiple layers of formvar stretched over 25 μm diameter Wolfram support wires. These windows are constructed on removable frames which fit on a special cover plate for the counter, as shown in Fig. 1 and 2. The support wires are wound on a jig and are then epoxied in place. After the epoxy has set the excess wire is removed and successive layers of formvar are applied over the wires and allowed to dry; no adhesive is used. Each formvar layer is a double thickness (2.4 to 3.0 $\mu g/cm^2$ total) obtained by lifting a formvar film from a water surface with a vertically oriented wire loop. Finally, a thin coating of gold is evaporated onto the rear of the window to provide a conducting surface which serves as the front cathode of the proportional counter.

A number of these windows were carefully destroyed to determine the bursting pressure as a function of support-wire spacing and window thickness. It was found that the pressure at which the foils rupture is proportional to the window thickness and inversely proportional to the wire spacing and also that the pressure at which the wires break is inversely proportional to the wire

* Evanohm S, W.B. Driver Co., Newark, N.J.--10 μm dia., 186 Ω/cm.

spacing. The window opening was 2 cm in diameter. The thinnest foil tested (50 $\mu g/cm^2$ thickness with 1.25 mm wire spacing, i.e. 98% transmission) could be operated safely at a gas pressure of 0.1 atm. The average results of these tests are summarized in Fig. 3.

3. Position Determination

The horizontal position information (position along the wire) is extracted using resistive charge division techniques.[3] The fraction of the total charge induced on the wire that is collected at one end is linearly related to the position when low impedance preamplifiers are used on each end of the wire. The wire resistance is rather low, about 950 ohms, but this poses no special problems. With such a short counter analog circuits may be used to perform the necessary division to compute the position without incurring any loss of accuracy.

The vertical position information (distance normal to he wire) is extracted by measuring the time difference between the arrival of the signals from the proportional counter and the stopping detector. The time delay of the proportional counter pulse, several hundred nanoseconds, is due to the transit time of the primary ionization electrons from the particle path to the anode wire. This time difference will be linearly related to the vertical position only if the drift velocity of the electrons is independent of electric field strength.

4. Performance

4.1 Position Performance

A drift time spectrum of 9 MeV ^{12}C ions passing through a mask of 0.7 mm wide horizontal slits is shown in Fig. 4. For this situation, covering much of the detector, the nonlinearity of the response is apparent in the fact that the peaks are most closely spaced near the center of the opening and more widely spaced both in the high field region near the anode wire and the low field region far from it. This behavior is qualitatively consistent with the known variation of drift velocity with field strength for P-10 (90% argon + 10% methane).[4] The peaks are all about 1 mm FWHM.

More detailed tests were performed using a ^{241}Am alpha source collimated to produce five lines approximately 0.4 mm wide and 2.5 mm apart. In addition to P-10, pure CH_4 (methane) and C_3H_8 (propane) were used. Typical two dimensional position spectra are shown in Fig. 5 for two orientations of the source; the resolutions obtained for the three gases, all at about 0.1 atm pressure, are summarized in Table 1. The numbers quoted include the contribution of the source slit. Subtraction of this effect leads to intrinsic detector resolution of substantially less than 0.4 mm for C_3H_8 and CH_4.

The C_3H_8 results are clearly superior for the operating conditions chosen. For the CH_4 tests, the anode voltage was adjusted to give roughly three times the amplification as was used in the C_3H_8 tests; this gave the same pulse height since the primary ionization was about one third as large. For P-10 the counter was biased just below the point at which it became unstable; the amplification was one half to one third that used in the C_3H_8 tests. We

believe that the loss of resolution at high gains is due to erratic spreading of the avalanche caused by run-a-way photon production. The present data support this conclusion to the extent that the drift time resolution, which is mostly sensitive to the "leading edge" of the avalanche, is consistently better than the charge division resolution which is equally sensitive to all phases of the avalanche production. Further, the charge division spectra for P-10 show a background of events well away from the peak which is presumably caused by large excursions of the avalanche from its origin. Finally it was noted that the charge division resolution deteriorated even for C_3H_8 when biased to give about four times as much amplification. Thus, it may be that all three gases can give similar results but that some must be used at lower multiplications than others.

The drift time versus position responses of the three gases obtained from data such as that of Fig. 5 are plotted in Fig. 6. The region shown is the middle one centimeter of the active area. The response for C_3H_8 shows the largest deviation from linearity. For the case of CH_4, drift velocity data[4] indicates that P-10 will show a larger deviation from linearity than CH_4 in the unobserved high field region of the detector. The relative drift velocities are consistent with reported values[4] and correspond to a considerable saturation of the drift velocity.

4.2 Energy Loss Resolution

A ΔE spectrum for 9 MeV ^{12}C recoils produced by 40 MeV α particles is shown in Fig. 7. A mono-energetic group was selected by requiring coincidence between the telescope and a detector at the kinematically appropriate angle for the scattered α particle.

The resolution of 8% FWHM, contains a contribution from 4% energy loss straggling, leaving an intrinsic resolution of 7% for the proportional counter. Such resolution is adequate to separate elements up to $Z \approx 10$.

4.3 Total Energy and Time Resolution

The overall energy resolution of the telescope is governed by the intrinsic resolution of the stopping detector, the energy loss straggling in the window and the intrinsic resolution of the proportional counter ($\sim 0.07 \times \Delta E$). The relative importance of the various contributions depends greatly on the particle being detected and the choice of window thickness and gas pressure. Generally, however, optimum choices can be made such that the dominant contribution is from the stopping detector. The time resolution is also determined by the stopping detector and can be quite good,[5] certainly $\lesssim 100$ ps. The telescope operates well up to 10 kHz but at higher rates pulse pile-up becomes a problem for both the ΔE and E signals.

5. Applications

The device has been used in a $^{12}C(\alpha,\alpha')^{12}C$ experiment[6] where the scattered alphas leaving ^{12}C in its 7.65 MeV state and the corresponding ^{12}C recoils are detected in coincidence; the very small radiative decay branching ratio of the state ($\sim 4 \times 10^{-4}$) is then given by the ratio of number of coincident events to the number of α single events leading to population of the state. In order tc reduce backgrounds and ensure full efficiency it was convenient to use a counter telescope which could identify the 9 MeV recoils and measure their spatial distribution.

A rather different application is the detection of fission fragments. Figure 8 shows a ΔE-E spectrum following ^{3}He induced fission of ^{238}U.[7] The fission fragments are very clearly separated from the light elements and the window is sufficiently thin so that the energy spectrum is not seriously distorted. (The maximum energy loss of ^{90}Zr ions in 100 $\mu g/cm^2$ of ^{12}C is about 6 MeV.) Use of the two dimensional position information here would make measurements of in and out of plane correlations relatively easy and efficient.

Other applications in which this detector might be valuable include: the measurement of two dimensional blocking or channeling patterns, detection of low energy particles from the decay of resonances and detection of reaction products with compensation for energy changes with angle.

6. Linearizing the Drift Time Readout

In applications where good linearity is required for both position coordinates, the problem of rapid field decrease in the drift direction must be dealt with. A number of electrode geometries have been considered using relaxation calculations to determine the electric field. Repelling (negatively charged) electrodes placed opposite to the anode wire lead to an unacceptable loss of charge, since electrons at the ends of the tracks are pushed into the cathode walls. Additional anode structures which do not collect charge do not influence the fields significantly while the addition of more amplifying wires introduces gain matching problems. Two changes do have beneficial effects. One is to make the proportional chamber deeper and the other is to use a larger diameter anode wire. The deeper chamber reduces the rate

of decrease of the field and the larger wire simply raises the field strengths everywhere.

These changes might make it desireable to find a different readout technique for the horizontal coordinate because high resistance large diameter wire is not conveniently available and, because in a very deep chamber, it may be desireable to use only the first electrons reaching the anode for the position determination. This could be done by inducing charge onto a delay line, either directly[1,8] or through pickup electrodes.[9] The simplicity of the counter can be more-or-less preserved by using compact, commercially available lines of either the distributed or lumped constant type.

7. Conclusions and Summary

The characteristics of the counter can be summarized as:

1) Simple construction-three machined parts
2) Ultra-thin windows and ΔE counter to accommodate E/M>0.2 MeV/amu
3) ΔE resolution $\tilde{\sim}$7% + straggling
4) Total energy and time resolution characteristic of a surface barrier detector
5) Position sensitivity in two dimensions with an accuracy <0.4 mm FWHM
6) Active area 400 mm^2, limited by the size of the surface barrier detector.

Gas fillings of P-10, CH_4 and C_3H_8 have been studied. For linearity of drift time response CH_4 is recommended. However C_3H_8 is recommended when high gain and stopping powers are needed for less ionizing particles. Possibilities for further linearizing the drift time response were discussed.

We gratefully acknowledge the assistance of D. Johnson in the field calculations.

TABLE 1.--Position resolutions[a] for various gases.

	Line Widths (mm FWHM)	
	ΔX^b	ΔY^b
P-10	0.80	0.61
CH_4	0.63	0.45
C_3H_8	0.47	0.46

a) Measurements done with ^{241}Am alpha particles collimated to produce lines about 0.4 mm wide and at a gas pressure of about 0.1 atm.

b) X is determined by charge division; Y is determined by drift time.

References

1. A. Breskin, G. Charpak and F. Sauli, Nucl. Instr. and Meth. 125, 321(1975).
2. H. Sann, H. Damjantschitsch, D. Hebbard, J. Junge, D. Pelte, B. Povh, D. Schwalm and D.B. Tran Thoai, Nucl. Instr. and Meth. 124, 509(1975).
3. G.L. Miller, N. Williams, A. Senator and R. Stensgaard, Nucl. Instr. and Meth. 91, 389(1971) and H.W. Fulbright, R.G. Markham and W.A. Lanford, Nucl. Instr. and Meth. 108, 125(1973).
4. T.E. Bortner, G.S. Hurst and W.G. Stone, Nucl. Instr. and Meth. 28, 103(1957).
5. B. Zeidman, W. Henning and D.G. Kovar, Nucl. Instr. and Meth. 118, 361(1974).
6. R.G. Markham, S.M. Austin and M.A.M. Shahabuddin, to be published
7. W.A. Lanford, E. Kashy, B.H. Wildenthal and R.G. Markham, private communication.
8. D.M. Lee, S.E. Sobottka and H.A. Thiessen, Nucl. Instr. and Meth. 109, 421(1973).
9. R.G. Markham and R.G.H. Robertson, to be published in Nucl. Instr. and Meth. and E. Beardsworth, J. Fischer, S. Iwata, M.J. Levine, V. Radeka and C.E. Thorn, to be published in Nucl. Instr. and Meth.

Figure Captions

Figure 1.--Schematic cross section of the counter: (a) window frame, (b) front cover plate (c) surface barrier detector, (d) Microdot-to-Microdot bulkhead feedthrough, (e) anode wire, (f) window.

Figure 2.--Photograph of the counter with the front cover plate and window frame removed. Also shown at the far right is a cover plate for thick windows.

Figure 3.--Summary of the window bursting tests. The graph shows the minimum areal density σ_{min} needed to support a given pressure P for various support wire spacings. The curves are labeled according to the transmission T of the support wire array and terminate when the pressure is sufficient to break the wires. The formulae give the minimum area density σ_{min} as a function of P and T and the maximum transmission T_{max} as a function of P.

Figure 4.--Drift time spectrum of 9 MeV ^{12}C ions passing through a set of slits 0.7 mm wide, 2.5 mm apart and parallel to the anode wire. The gas filling was P-10 at 0.1 atm.

Figure 5.--Two dimensional position spectra for two orientations of a ^{241}Am alpha source collimated to produce five lines approximately 0.4 mm wide and spaced 2.5 mm apart. The vertical position Y is determined by drift time and the horizontal position X by charge division. The gas filling was CH_4 at 0.1 atm.

Figure 6.--Drift time versus position over the central region of the counter for the three gases tested. The drift time is 1.6 nsec/channel.

Figure 7.--Energy loss spectrum of 9 MeV ^{12}C target recoils produced by $^{12}C(\alpha,\alpha)$. Coincidence with any scattered alpha at the kinematically appropriate angle was required. The low pulse height events are due to breakup particles induced by inelastic scattering to unbound states. The ΔE resolution is 8% FWHM.

Figure 8.--A ΔE-E spectrum of fission fragments from a 76 MeV ^{3}He induced fission of ^{238}U. The fragment events in the upper part of the figure are clearly resolved from light element events which appear in the lower left hand corner.

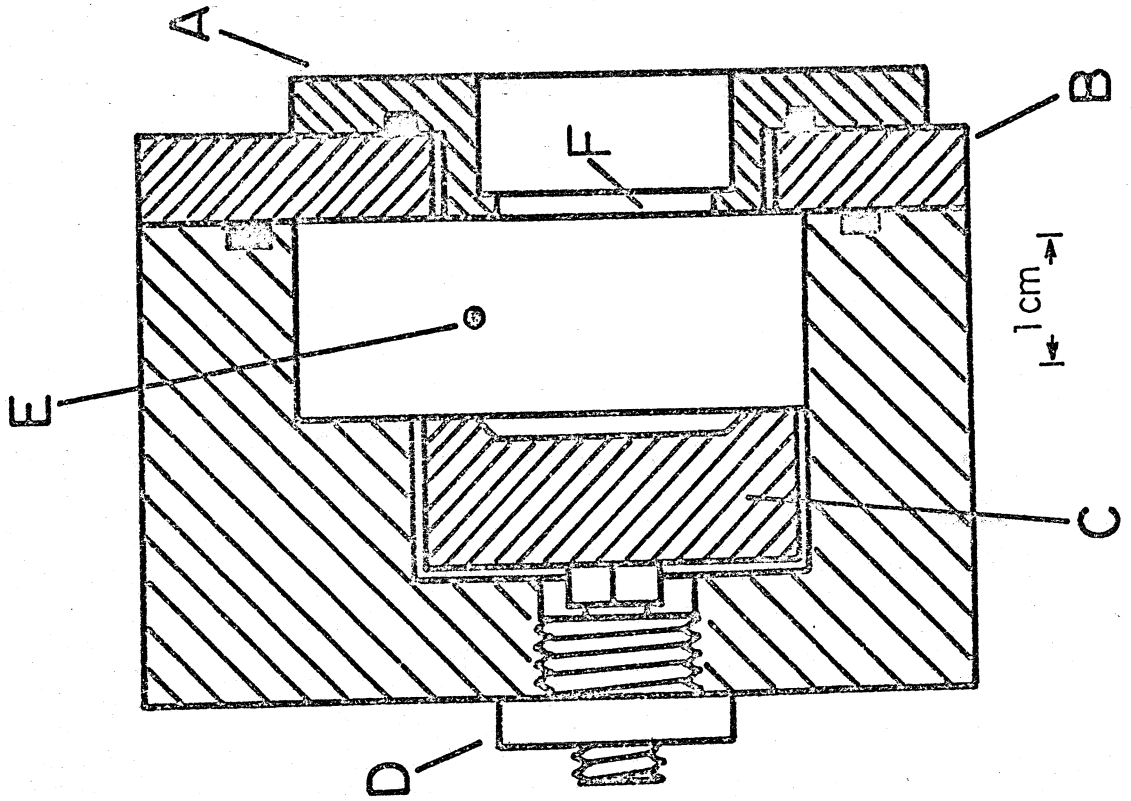

Fig. 1

15

16

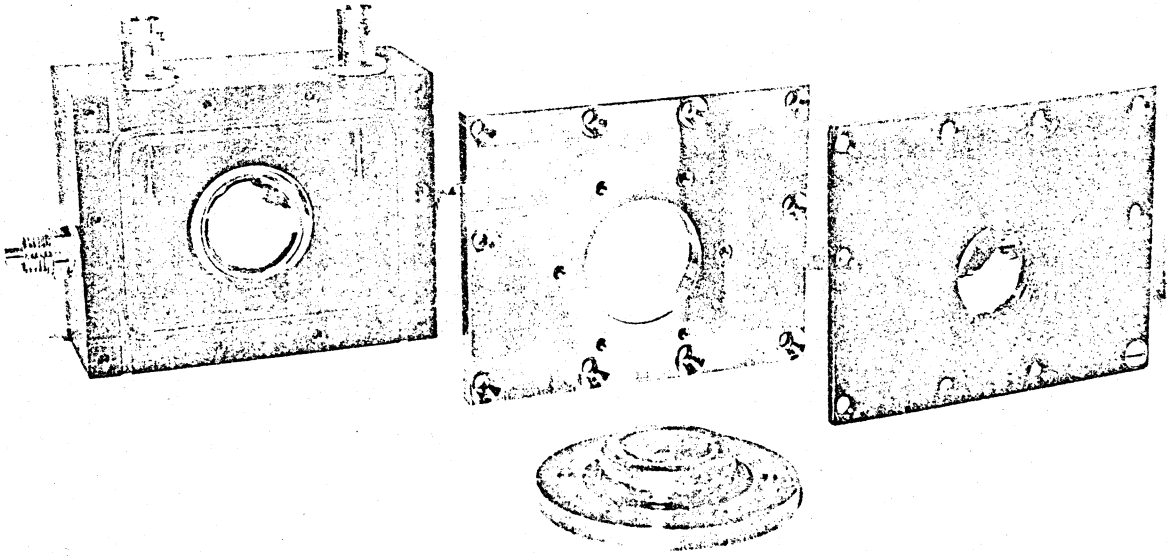

Fig. 2

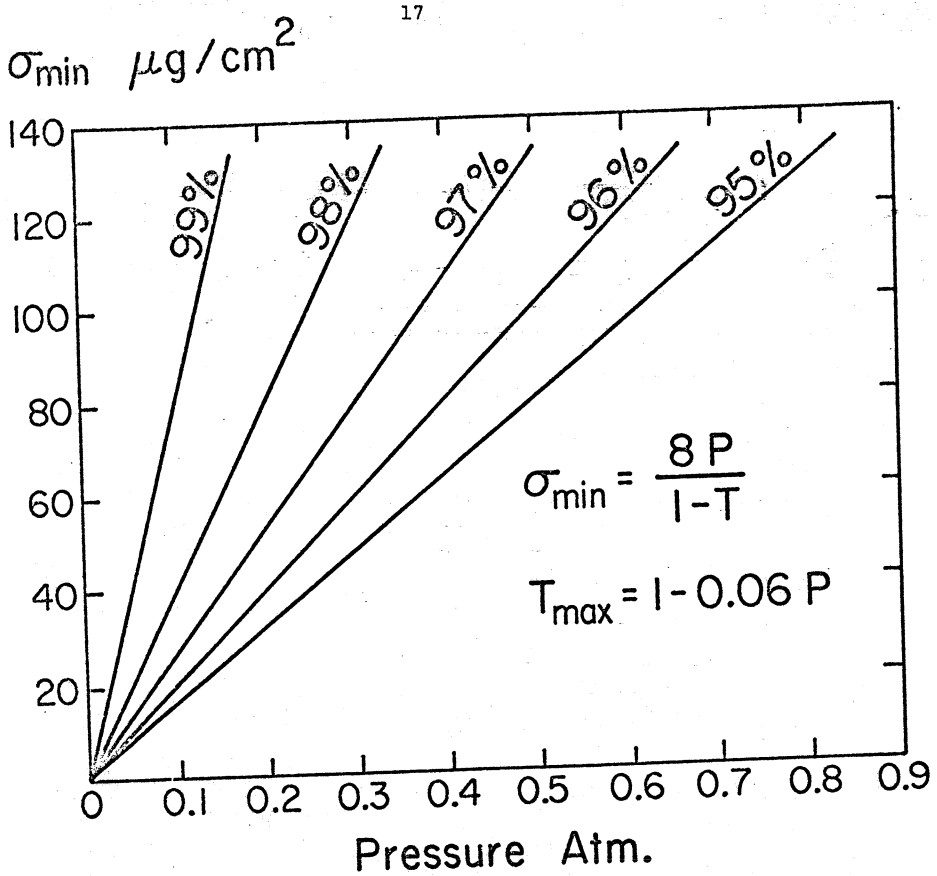
σmin μg/cm²
140
120
100
80
60
40
20
99%
98%
97%
96%
95%
σmin = 8 P / 1-T
Tmax = 1-0.06 P
0
0.1
0.2
0.3
0.4
0.5
0.6
0.7
0.8
0.9
Pressure Atm.

Fig. 3

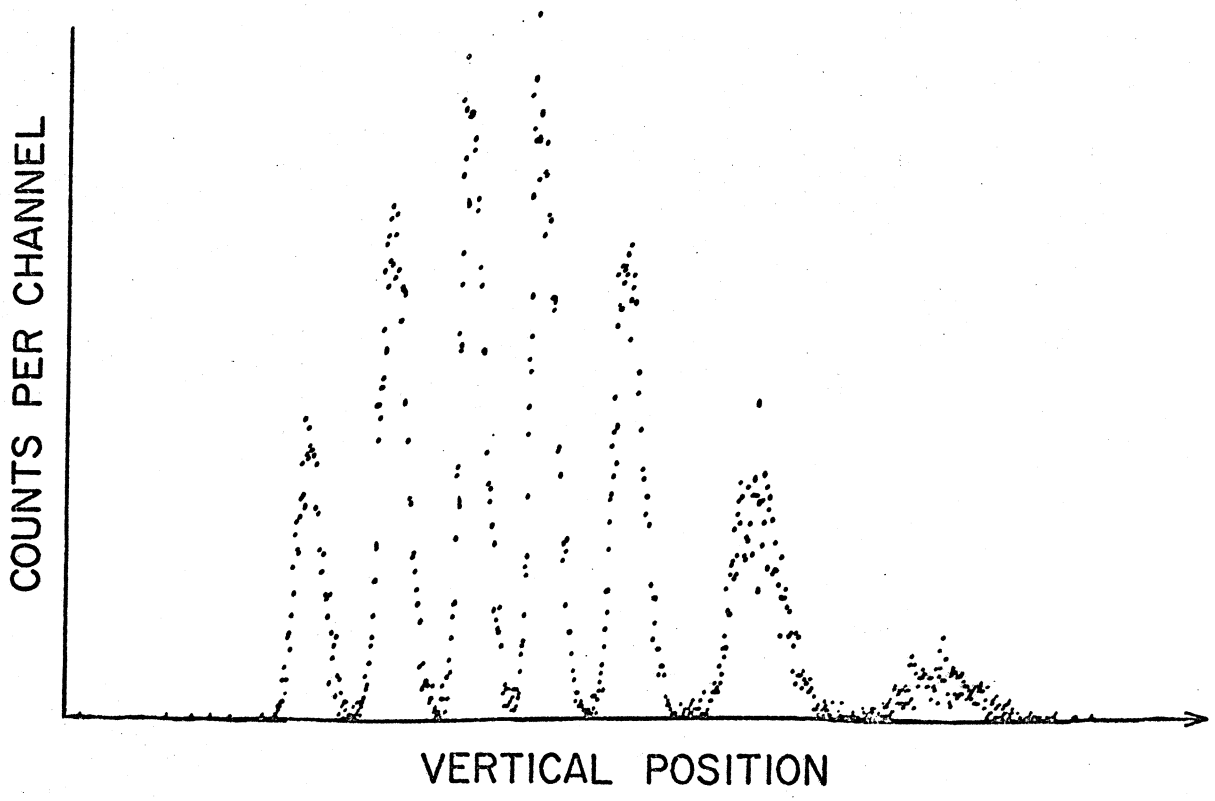
COUNTS PER CHANNEL
VERTICAL POSITION

Fig. 4

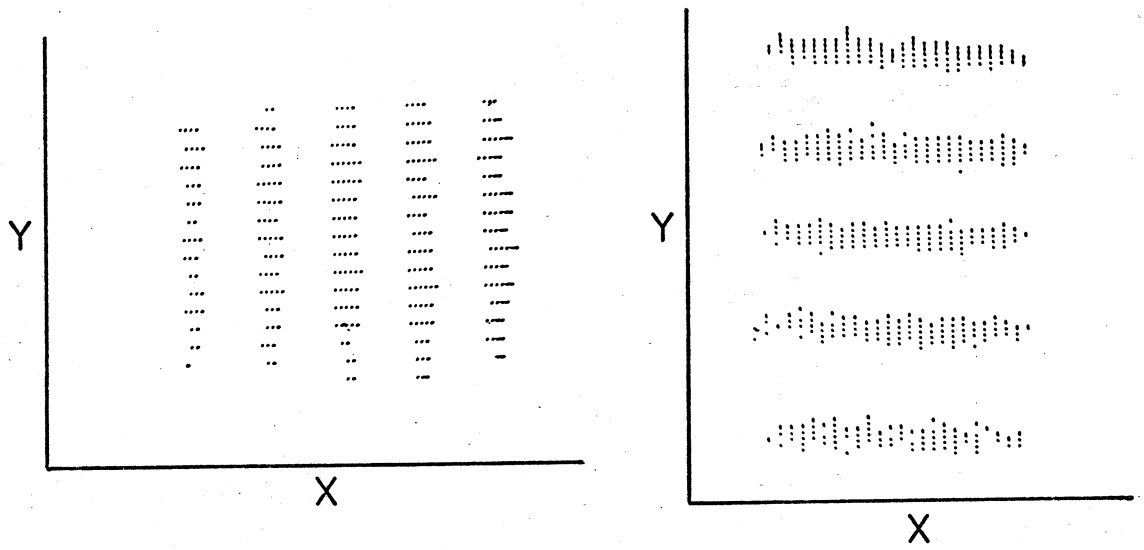
Y
X
Y
X

Fig. 5

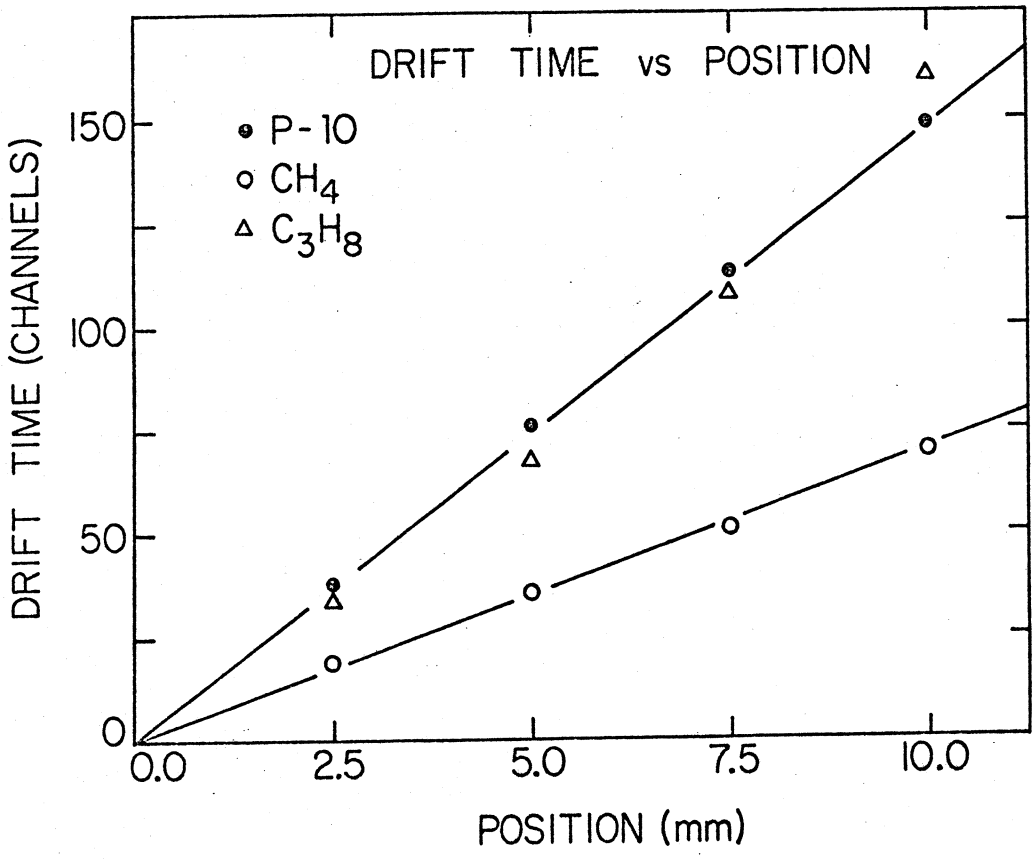
DRIFT TIME vs POSITION
P-10
CH4
C3H8
DRIFT TIME (CHANNELS)
150
100
50
0
0.0
2.5
5.0
7.5
10.0
POSITION (mm)

Fig. 6

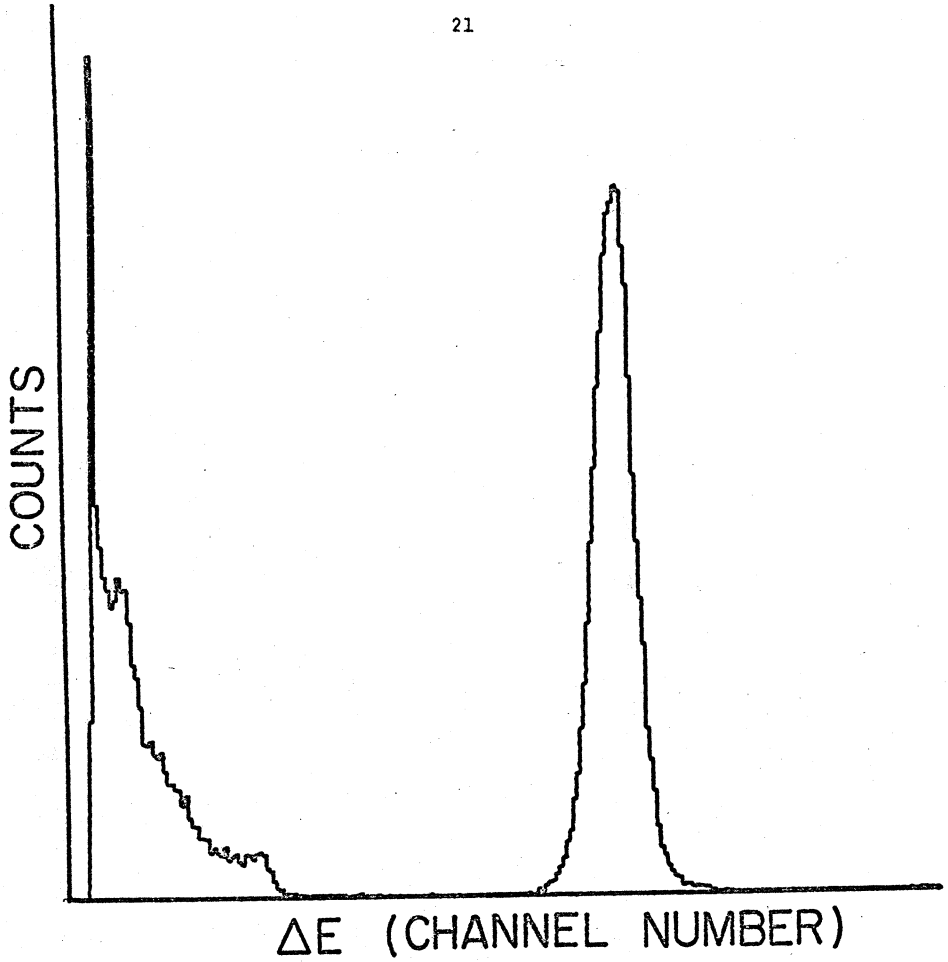
COUNTS
ΔE (CHANNEL NUMBER)

Fig. 7

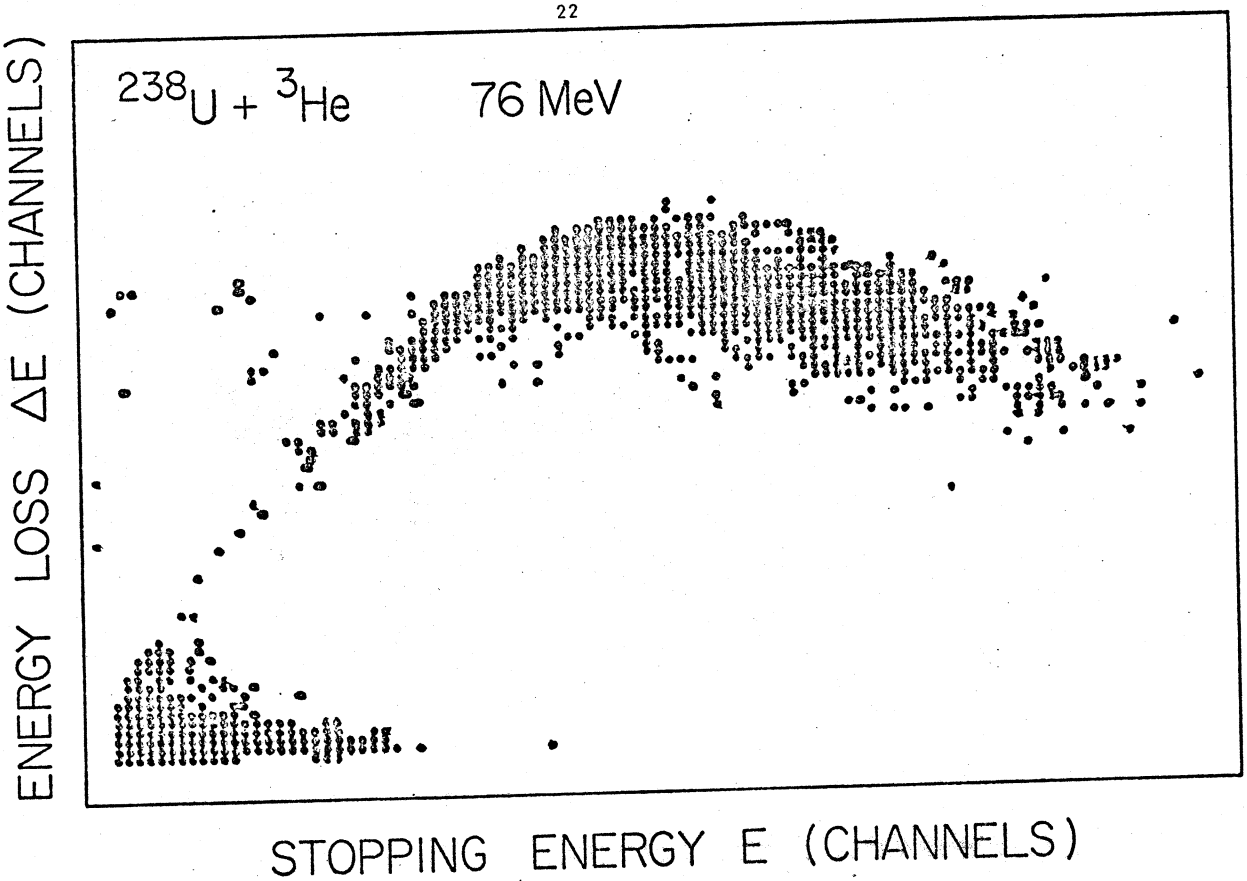
$^{238}U + ^{3}He$ 76 MeV
ENERGY LOSS ΔE (CHANNELS)
STOPPING ENERGY E (CHANNELS)

Fig. 8